RESISTIVE SENSOR FOR HIGH POWER MICROWAVE PULSE MEASUREMENT OF TE$_{01}$ MODE IN CIRCULAR WAVEGUIDE

Ž. Kancleris, G. Šlekas, V. Tamošiūnas, and M. Tamošiūnienė

Microwave Laboratory
Semiconductor Physics Institute
11 A. Goštauto, Vilnius 01108, Lithuania

Abstract—A resistive sensor (RS) devoted for high power microwave pulse measurement in cylindrical waveguide is considered. The modeling results of the interaction of the TE$_{01}$ (H$_{01}$) wave with a semiconductor plate with contacts on sidewalls of the plate placed on a wall of the circular waveguide are presented. A finite-difference time-domain (FDTD) method was employed for the calculation of the electromagnetic field components, reflection coefficient from the semiconductor obstacle, and the average electric field in it. The features of the resonances have been used to engineer the frequency response of the RS. It has been found that such electrophysical parameters of the plate can serve as the prototype of the sensing element (SE) for the circular waveguide RS with flat frequency response.

1. INTRODUCTION

At present, different types of pulsed high power microwave (HPM) oscillators and amplifiers are being researched in laboratories, as well as manufactured by industry. They are used in communication systems, radars, electromagnetic testing facilities, scientific research, and military projects. Currently, the main device being used for the measurement of HPM pulse power is a semiconductor diode. However, when it is used to measure HPM pulses, the initial pulse has to be strongly attenuated. Large attenuation of the microwave power results

---

Corresponding author: Ž. Kancleris (kancleris@pfi.lt).

in a decrease of the measurement accuracy. In addition, the size and weight of the measurement system increase, and its control becomes complicated.

An alternative device for the HPM pulse measurement — the RS, performance of which is based on the electron heating effect in semiconductors, has been developed in [1]. The electric field of the microwave pulse heats electrons in the SE placed in the waveguide, and its resistance increases. By measuring this resistance change the microwave pulse power in the transmission line is determined. The RS can measure HPM pulses directly, produces high output signal, is overload resistant, and demonstrates very good long term stability [1]. The RS developed for rectangular waveguides are used in laboratories dealing with HPM pulses worldwide. Unfortunately, so far as we know, the RS for the circular waveguide has not been designed yet, and it is the object of our investigation.

Although the TE_{01} mode propagating in circular waveguide is not the lowest one, it is used in the design of microwave devices because it is a mode, whose losses decrease with increasing frequency [2]. The low-loss TE_{01} mode in circular waveguide has been utilized for several decades. It was used in several applications including communication systems, antenna feeds and RF systems for high-energy accelerators [3]. The currents associated with TE_{01} modes are in the circumferential direction only, and this property can be used to construct mode filters [2]. For example, a novel circular TE_{01} mode bend for HPM applications is presented in [3]. The bend has very low ohmic losses, and the TE_{01} mode is transmitted with virtually perfect mode purity. The characteristics of a 35-GHz oscillator operating with the TE_{01} circular waveguide mode are described in [4]. The gyrotron was specially designed as a source for electron cyclotron heating experiments.

The main goal of this paper was to investigate the interaction of the electromagnetic wave, propagating in the circular waveguide, with the n-Si plate placed on the waveguide wall and to find such electrophysical parameters of the plate that it could serve as the prototype of the SE for the circular waveguide RS for TE_{01} mode that is used in HPM experiments.

2. THE RESISTIVE SENSOR IN A CIRCULAR WAVEGUIDE

A plate with the contacts on sidewalls of the plate in the circular waveguide was analyzed in this paper. The practical realization of the design of the SE is depicted in Fig. 1(a). It is seen that the SE is simply

(a)   (b)
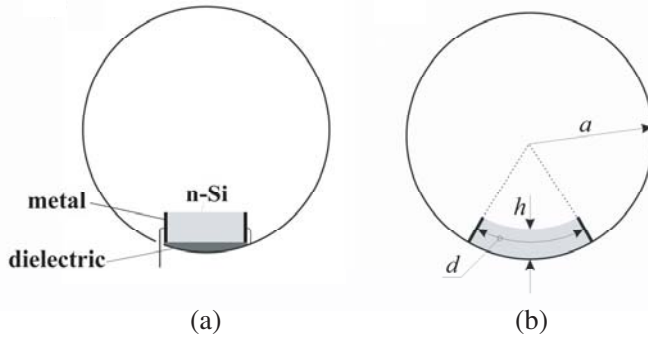
Figure 1. The practical realization of the SE in the circular waveguide (a) and its model in a cylindrical coordinate system (b).

laid on the isolating dielectric on the wall of the waveguide. One of the contacts of the SE is grounded, while the other one is isolated from the waveguide and is used for the RS feeding and the output signal measurement. Cross-sectional view of the investigated structure in a cylindrical coordinate system is shown in Fig. 1(b). In the model of the SE the metal contacts are perpendicular to the direction of the electric field E_φ in the regular wave.

The main requirements for the SE could be formulated as follows: first, the SE should not insert considerable reflection in the waveguide, so the value of VSWR has been set at <1.2; second, the RS should be able to measure nanosecond-duration HPM pulses; therefore, the DC resistance of the RS should not exceed $50\,\Omega$; third, the shape of the SE should be taken as a plate that is important for heat transfer from the SE; finally, the flat frequency response of the RS in the waveguide's frequency band is preferable.

2.1. FDTD Method

We have used the FDTD method for the calculation of the electromagnetic field components [5, 6]. The advantages of FDTD method are accented in [7, 8]; it was mentioned that FDTD is widely regarded as one of the most popular computational electromagnetics algorithms. In [9–15], FDTD method was applied to compute the propagation characteristics of cylindrical transmission lines.

The modeled section of the waveguide with the SE analyzed in this paper is shown in Fig. 2. We used a cylindrical coordinate system and dimensionless coordinates and time: r/a, z/a, $t \cdot c/a$ where c is the velocity of light in free space and a is a radius of the waveguide.

(a)   (b)
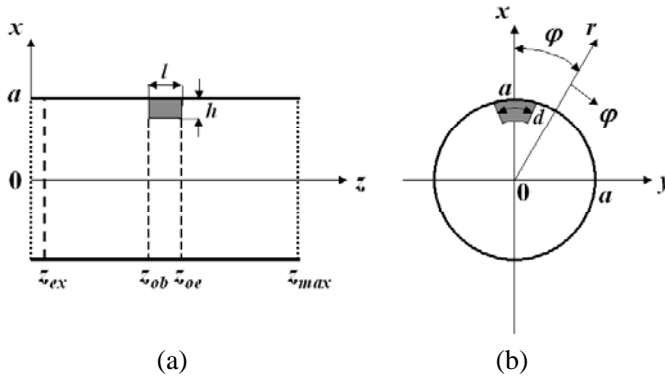
Figure 2. The sectional view of the modeled circular waveguide with obstacle in $x0z$ plane (a) and $x0y$ plane (b).

In the plane $z = z_{ex}$, the TE_{01} type wave is excited. It propagates into both sides from the excitation plane. The obstacle is placed at one wavelength in the waveguide ahead from the excitation plane and at the same distance before the right side of the modeled waveguide section. In the planes $z = 0$ and $z = z_{max}$ non reflecting absorbing boundary conditions are satisfied. Therefore, the waves traveling left from the excitation plane as well as reflected from the semiconductor obstacle are absorbed in the plane $z = 0$, whereas the wave passing the semiconductor structure is absorbed in the plane $z = z_{max}$. Due to the reflection from the semiconductor obstacle the partly standing wave is formed between planes $z = z_{ex}$ and $z = z_{ob}$. From the amplitude distribution in this area, the reflection coefficient was determined.

The cutoff frequency of the TE_{01} mode propagating in the circular waveguide is twice of that for the lowest TE_{11}. The regular TE_{01} wave has only three components: E_φ, H_r and H_z [16]. However, in a vicinity of the SE all electromagnetic field components might appear. Therefore, Maxwell's equations have to be solved by computing all six components of the electric and magnetic fields to determine the average electric field amplitude in the semiconductor obstacle. Using dimensionless variables and measuring up the magnetic field strength in electric field units $Z_0 H$, where Z_0 is an impedance of free space, Maxwell's equations in the semiconductor obstacle can be written in

the following way

$$\frac{\partial \mathbf{E}}{\partial t} = (\nabla \times \mathbf{H} - \gamma \cdot \mathbf{E})/\varepsilon_r, \qquad (1)$$

$$\frac{\partial \mathbf{B}}{\partial t} = -(\nabla \times \mathbf{E}). \qquad (2)$$

There $\gamma = Z_0 \cdot a \cdot \rho$ accounts for losses in the structure. Here ρ and ε_r are the specific resistance and relative dielectric constant of the semiconductor obstacle; it was assumed that $\mu_r = 1$ for the entire simulation area. Outside the obstacle $\gamma = 0$ and $\varepsilon_r = 1$.

The grid of points where the particular component is computed is shifted at a half of a step with respect to each other as it was proposed in [5]. Moreover, electric and magnetic fields are calculated at different time moments providing h^2 accuracy in the calculation both space and time derivatives. The details of the application of this technique to the cylindrical coordinate system can be found in the monograph [6].

The grid can be chosen in such a way that it starts and finishes with the points where the electric field components should be calculated. For the investigated frequency range real metals can be sufficiently precisely simulated using so called perfect electric conductor approximation, which assumes that tangential electric field components are simply zeroed on the metal surface. Therefore, the components E_φ and E_z are zeroed on the waveguide walls. Also, the grid has been chosen in such a way that tangential electromagnetic field components were located in the contact plane and therefore zeroed during FDTD update. For configuration of the SE investigated here, E_r and E_z components of the electric field are set to zero on the metal contacts. In the planes $z = 0$ and $z = z_{\max}$ non reflecting boundary conditions for the components E_r and E_φ are satisfied.

At $t \leq 0$ there are no electromagnetic fields in the modeled section of the waveguide; therefore all components of the electric and magnetic field are set to zero. When the dimensions of the semiconductor obstacle is much less than the characteristic dimensions of the waveguide, its influence on the wave propagating in the waveguide is comparatively small. In such a case, the stationary solution is achieved faster when the waveguide is filled with ordinary components of the TE$_{01}$ wave. Choosing the time step Courant criterion formulated for 3-D cylindrical coordinate FDTD procedure in [10] has to be taken into account.

Some of the components of the electromagnetic field, namely H_r, E_φ, and E_z, cannot be straightforwardly computed at $i = 0$ ($r = \triangle r \cdot i$, where $\triangle r$ is the cylindrical coordinate step and i is step number. This fact is known as the numerical singularity of a FDTD scheme in

cylindrical coordinates at $r = 0$ [6]. A variety of numerical procedures dealing with the singularity have been proposed. More widely an integral form of Maxwell equations near $r = 0$ [11, 12] and the series polynomial expansion in the radial direction [13, 14] have been used to resolve the problem. We have followed the simple method proposed in [15] and based on the use of the Cartesian coordinate system in the vicinity of $r = 0$.

The program computing the electromagnetic field components was written using C++ programming language. The suitability of the program has been proved in [17] where computations results were tested by comparing ones with the analytical solution.

2.2. Sensitivity

We consider a sensitivity of the RS in the linear region where the output signal is proportional to the pulse power P propagating in the waveguide. Since the resistance change of the SE is the quantity indicating pulse power in the waveguide, it is convenient to define the sensitivity of the RS as

$$\zeta = \frac{\Delta R/R}{P} = \frac{\beta^* \langle E \rangle^2}{P}. \tag{3}$$

There $\Delta R/R$ is a relative resistance change of the SE in the microwave electric field; β^* is an effective warm electron coefficient defining deviation of the current-voltage characteristic from Ohm's law [1]; and $\langle E \rangle$ is an average of the electric field amplitude in the SE.

Inserting into (3) the expression defining power propagating in the circular waveguide one can get the following expression, describing the sensitivity of the RS in the linear region:

$$\zeta = \frac{2\beta^*}{\pi a^2} \left[\frac{J_1(\chi_{11})}{J_0(\chi_{01}))} \right]^2 \frac{Z_0}{\sqrt{1 - (f_c/f)^2}} \left(\frac{\langle E \rangle}{E_0} \right)^2, \tag{4}$$

where f and f_c are the frequency of electromagnetic oscillations and the cutoff frequency for the TE_{01} mode, respectively; J_0 and J_1 are the corresponding order first kind Bessel functions; $\chi_{01} = 3.832$ is the root of J_1; $\chi_{11} = 1.841$ is its first derivative root; and E_0 in the obtained expression denotes the maximum of the electric field amplitude in the regular TE_{01} wave in the empty waveguide.

Making use of the empirical relation [1] to describe the resistance change of the SE over a wider range of electric field, the following expression can be obtained relating relative resistance change with

pulse power transmitted through the waveguide:

$$\frac{\Delta R}{R} = \frac{1}{2k_n^*} \left[\sqrt{1 + \frac{8k_n^*\beta^*}{\pi a^2} \left[\frac{J_1(\chi_{11})}{J_0(\chi_{01}))} \right]^2 \frac{Z_0 \cdot P}{\sqrt{1 - (f_c/f)^2}} \frac{\langle E \rangle^2}{(E_0)^2}} - 1 \right],$$
(5)

where additional coefficient k_n^* describes the deviation of $\Delta R/R$ from quadratic dependence. In the limit $P \to 0$, (5) expression goes over into (4).

The average electric field is the only unknown quantity in (4) and (5). Thus determining it the sensitivity of the RS in the linear region and the dependence of $\Delta R/R$ on power in a wider dynamical range can be calculated.

3. NUMERICAL RESULTS AND DISCUSSION

Calculations were performed for the circular waveguide radius of which $a = 20\,\text{mm}$, the electric field amplitude was normalized to the maximum of the electric field amplitude of the regular wave in the empty waveguide E_0.

3.1. Resonances

Although the dimensions of the SE are much less than the wavelength of the electromagnetic oscillations, due to large value of $\varepsilon_r = 11.9$ some resonance phenomenon may occur in it. We have analyzed the influence of the length l, height h and width d of the dielectric SE on the resonance position by changing one of the dimensions of the obstacle while the other dimensions were fixed.

The usual resonance shift to the lower frequency was obtained when the length l of the SE is growing, because the larger wavelength wave fits the increased length of the sample. Calculated dependencies of the average electric field component E_φ in the dielectric obstacle on frequency for the different height h and width d of obstacles are presented in Fig. 3. It is seen (ref. to Fig. 3(a)) that the increase of height h leads to the significant shift of the resonance to lower frequencies, while the increase of the width d (ref. to Fig. 3(b)) does not influence much resonance position. The E_φ is the major electric field component in the SE of such configuration. The height is the transverse dimension of the SE with respect to the direction of the electric field in this case. It is seen that the greatest influence on the resonance position has the dimension that is transverse with respect to the direction of the electric field dominating in the SE. Let us recall that
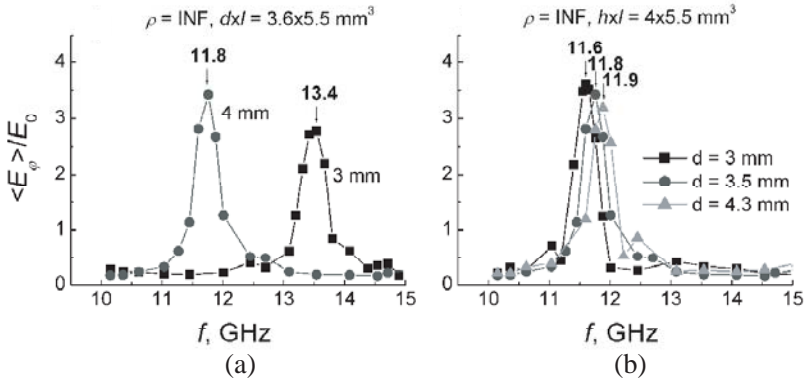
Figure 3. Calculated dependencies of the average electric field component E_φ in the dielectric obstacle on frequency for the different height h ($d \times l$=3.6×5.5 mm^2) (a), and width d ($h \times l$=4.0×5.5 mm^2)(b) of the obstacles. The positions of the resonance are specified in the figure.

the same peculiarity is the characteristic of the lowest TE wave TE_{10} in the rectangular waveguide. For example, the critical wavelength depends only on the transverse dimension of the waveguide window. It is worth noting that the position of the resonance in the frequency scale for the SE investigated here can be easily shifted by changing either the length or the height of the obstacle while the average electric field in it can be adjusted by changing specific resistance of the SE.

3.2. Electric Field Strength in SE

We started investigations from the smallest devices, where the influence of resonances can be avoided. Only very small amplitudes can be expected in high loss ($\rho = 2\,\Omega\cdot$cm) case. Situation is slightly improved for $\rho = 20\,\Omega\cdot$cm, since the amplitude increases by a factor of four approximately. However, the resistance of the RS increases to almost $100\,\Omega$ in this case that is substantially above the $50\,\Omega$ target. In addition, due to the boundary condition for the tangential field component near the metal surface E_φ should be zero on the waveguide wall. This substantially decreases the average electric field strength in the SE. During our investigations, we faced with the problem for all simulated smallest devices — there was no sufficient average electric field growth with frequency to compensate the sensitivity decrease caused by the wave dispersion in the waveguide (ref. to (4)). Therefore,

Table 1. The average electric field components for the different height SE. Dimensions of the SE: $d \times l = 1.8 \times 2\,\text{mm}^2$, $\rho = 20\,\Omega\cdot\text{cm}$, $f = 10.2\,\text{GHz}$.

	$h = 2\,\text{mm}$	$h = 4\,\text{mm}$	$h = 6\,\text{mm}$
$\langle E_r \rangle$	0.0009	0.0014	0.0011
$\langle E_\varphi \rangle$	0.2133	0.0950	0.0274
$\langle E_z \rangle$	0.0005	0.0010	0.0010
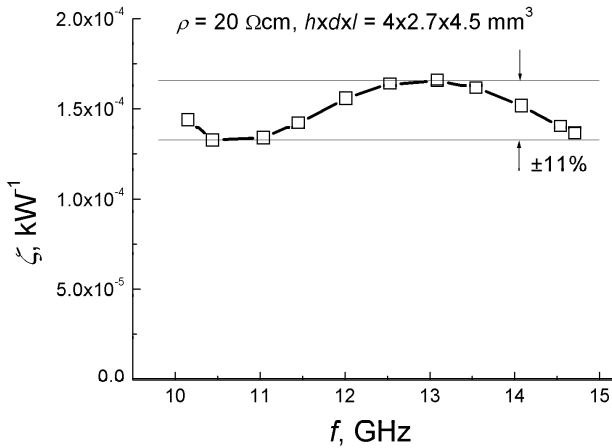
Figure 4. Calculated dependence of the sensitivity on frequency for the optimal RS. Dimensions of the SE are $h \times d \times l = 4 \times 2.7 \times 4.5\,\text{mm}^3$, $\rho = 20\,\Omega\cdot\text{cm}$, $a = 20\,\text{mm}$.

in order to obtain the optimized sensor substantially larger than 2 mm devices should be investigated. In this case, resonances can be constructively applied to "fix" the decrease of the sensitivity on frequency and increased l and h dimensions which lead to the decrease of the resistance of the RS at a fixed specific resistance.

We have also considered the dependence of the average electric field in the SE on its size and specific resistance. The increase of width of the SE has little influence on the amplitude of $\langle E_\varphi \rangle$ while the average electric field of the other two components increases. The growth of the height of the SE leads to the decrease of $\langle E_\varphi \rangle$. Results illustrating it are collected in Table 1. It is seen that $\langle E_\varphi \rangle$ decreases 7.8 times when the height of the SE was tripled.
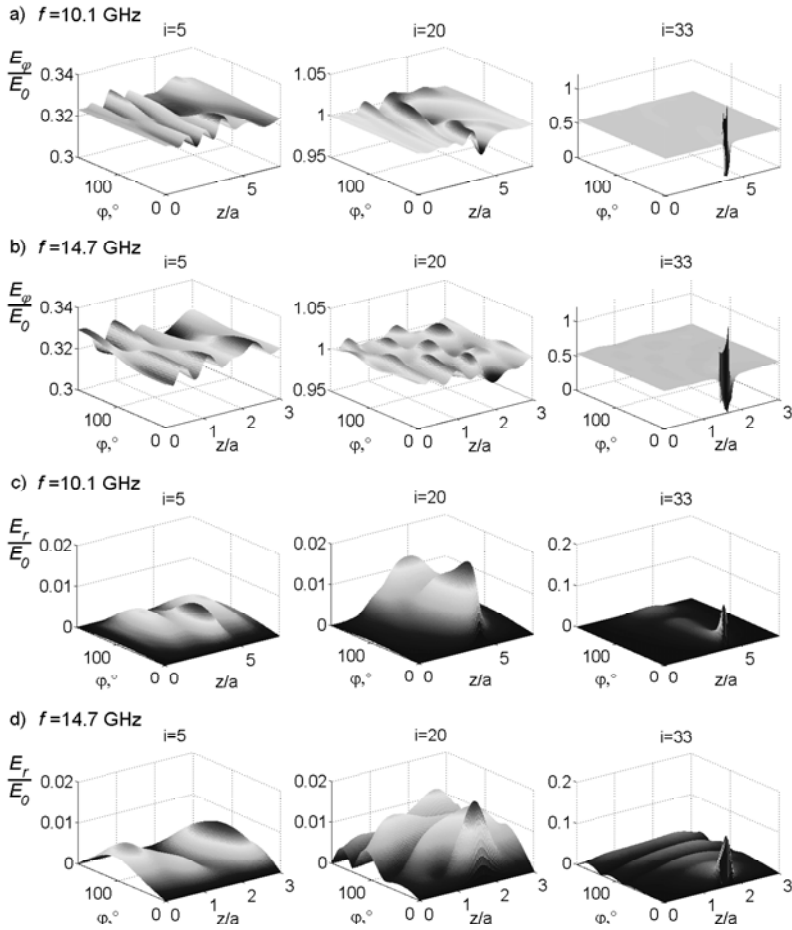
Figure 5. Distribution of the components of electric field in the waveguide with the optimal SE on the different surfaces $\varphi 0z$: E_φ at $f = 10.1$ (a) and $14.7\,\text{GHz}$ (b) for $r = (i-1) \cdot \Delta r$; E_r at $f = 10.1$ (c) and $14.7\,\text{GHz}$ (d) for $r = (i-0.5) \cdot \Delta r$; Calculation parameters: $\Delta r = 0.025$, $\Delta z = 0.025$, $\Delta \varphi = 1.4°$, $\Delta t = 3.05 \cdot 10^{-4}$. Dimensions of the SE are $h \times d \times l = 4 \times 2.7 \times 4.54\,\text{mm}^3$, $\rho = 20\,\text{cm}$, $a = 20\,\text{mm}$.

3.3. Optimized Frequency Response

Resonance investigation results presented in Fig. 3 suggest that for height $h = 4\,\text{mm}$ the length $l = 5.5\,\text{mm}$ is too large because the resonance occurs at $\sim 12\,\text{GHz}$. For our purposes it is better to get resonance at $13\,\text{GHz}$, or even above. Since the change of the width

does not influence the position of the resonance (ref. to Fig. 3(b)), one can shift the resonance to higher frequency by decreasing the length or the height of the SE. Unfortunately decrease of both l and h leads to the increase of the resistance of the sensor; therefore some compromise should be found. Considering factors influencing the resonance position it was found that an optimum resonance position can be obtained for the relatively short sample the length of which $l \leq 5\,\mathrm{mm}$. After estimating the optimum device size, several sets of simulations have been performed for similar sizes in order to determine the optimum specific resistance of the SE material.

Since the circular waveguide with TE_{01} mode is sometimes employed at a frequency close to cutoff frequency, let us consider frequency range $f_c/f = 0.9$ - 0.7. From (4) it is easy to get that the sensitivity in this frequency range decreases by a factor of 1.64. The increase of $\langle E_\varphi \rangle$ by a factor 1.28 is needed to compensate the decrease of the sensitivity due to wave dispersion in the waveguide. It turned out that the best results can be obtained for $\rho = 20\,\Omega$·cm material. The ratio of the average electric field amplitude $\langle E_\varphi \rangle$ at $f = 13.1\,\mathrm{GHz}$ to the $\langle E_\varphi \rangle$ calculated at $f = 10.2\,\mathrm{GHz}$ was determined for $h = 4\,\mathrm{mm}$ and for various l and d. From the calculation results, optimum ratio demonstrates the SE with transverse dimensions $d \times l = 3.5 \times 5\,\mathrm{mm}^2$. It was obtained that the sensitivity variation of the RS was $\pm 5\%$ within considered frequency range. Unfortunately, at higher frequency, sensitivity sharply decreases due to the decrease of the electric field strength in the SE with frequency. Therefore as an optimal device we choose the SE with the transverse dimensions $d \times l = 2.7 \times 4.5\,\mathrm{mm}^2$ that demonstrates flat frequency response in a wider frequency range. Its DC resistance is roughly $29\,\Omega$. The calculated dependence of the sensitivity on frequency is shown in Fig. 4. The value of $\beta^* = 9.3 \cdot 10^{-8}\,\mathrm{cm}^2/\mathrm{V}^2$ [1] was used in the calculations. The sensitivity variation within frequency range 10.1–14.7 GHz is $\pm 11\%$. It is the best result found now for the RS analyzed here. Although the height of the optimal SE is quite high, the RS does not perturb much the field distribution in a waveguide away from the RS. Calculated VSWR is practically independent of frequency and is lower than 1.05 within considered frequency range. The distribution of the components E_φ and E_r in the waveguide with the optimal SE for the lowest and highest considered frequencies are shown in Fig. 5. In the figure, the distribution of the components on the surfaces $\varphi 0z$ is presented within all modeled waveguide section. As one can see from the figure, the obstacle distorts the regular distribution of E_φ component of the TE_{01} wave. The largest perturbation is found on the surfaces closest to the obstacle. In the figure, the component E_r is excited in all modeled
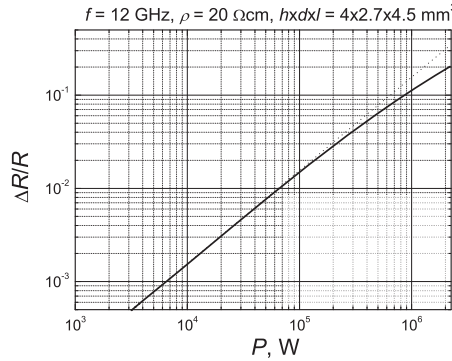
Figure 6. Calculated dependence of the relative resistance change of the optimal RS on power transmitted through the waveguide at $f = 12\,\mathrm{GHz}$. Dimensions of the SE are $h \times d \times l = 4 \times 2.7 \times 4.5\,\mathrm{mm}^3$, $\rho = 20$ Ω·cm.

waveguide section. However, its amplitude is very small in the central part of the waveguide. It becomes significant only near the obstacle. Comparing results presented in Fig. 5(c) and Fig. 5(d), one can see that the amplitude of E_r increases with frequency. It is worthwhile mentioning that the average electric field in the optimal SE mostly consists of the E_φ component. The E_φ increases from 0.07 to 0.1 in the considered frequency range. Average value of E_r is roughly 40 times, and E_z is more than 50 times less.

Once the electric field in the SE is determined the dependence of the relative resistance change on a power transmitted through the waveguide can be calculated using (5). The value of $k_n^* = 3.4$ was used in calculations [1]. The results are shown in Fig. 6 by a solid line. Dotted line corresponds to the linear dependence of $\Delta R/R$ on P that is characteristic of the warm electron region. It is seen that at a maximum power roughly 20% relative resistance change of the SE is observed.

Considering fitting of the frequency response in general, even better theoretical result may be expected for the precisely "tuned" d dimension. However, the differences between idealized and real devices should be considered before proceeding with fine-tuning of the parameters of the SE.

4. CONCLUSION

Our investigations have revealed that resonance phenomenon may occur even in sufficiently small obstacles placed in the cylindrical

waveguide. By shifting the resonance position the frequency response of the RS has been optimized. The optimal RS found at a moment should have the following electrophysical parameters: $\rho/a = 10\ \Omega$, $h/a \times d/a \times l/a = 0.2 \times 0.135 \times 0.225$. Calculated sensitivity variation within frequency range $f_c/f = 0.9$ - 0.62 for the optimal RS is roughly $\pm 11\%$, where f_c is the cutoff frequency for TE_{01} mode. Low DC resistance of $29\ \Omega$ is favorable for the impedance matching in the measurement circuit and sensor introduces only small reflections in the waveguide since its VSWR < 1.05 within the investigated frequency range.

ACKNOWLEDGMENT

REFERENCES

1. Dagys, M., Ž. Kancleris, R. Simniškis, E. Schamiloglu, and F. J. Agee, "Resistive sensor: Device for high-power microwave pulse measurement," *IEEE Antennas and Propagation Magazine*, Vol. 43, No. 5, 64–79, 2001.

2. Chatterjee, R., *Elements of Microwave Engineering*, John Wiley & Sons, New York, Chichester, Brisbane, Toronto, 1986.

3. Tantawi, S. G., "A novel circular TE_{01}-mode bend for ultra-high-power applications," *Journal of Electromagnetic Waves and Applications*, Vol. 18, No. 12, 1679–1687, 2004.

4. Read, M. E., M. Gilgenbach, R. F. Lucey, K. R. Chu, A. T. Drobot, and V. L. Granatstein, "Spatial and temporial coherence of a 35-GHz gyromonotron using the TE_{01} circular mode," *IEEE Trans. Microwave Theory and Tech.*, Vol. 28, No. 8, 857–878, 1980.

5. Kane, S. Y., "Numerical solution of initial boundary value problems involving Maxwell's equation in isotropic media," *IEEE Trans. Antennas Propagation*, Vol. 14, No. 3, 302–307, 1966.

6. Taflove, A., *Computational Electrodynamics: The Finite-*

difference Time-domain Method, Artech House, Norwood, MA, 1995.

7. Chew, W. C., J.-M. Jin, C.-C. Lu, E. Michielssen, and J. M. Song, "Fast solution methods in electromagnetics," *IEEE Trans. on Antennas and Propagation*, Vol. 45, No. 3, 533–543, 1997.

8. Chew, W. C., "A 3D perfectly matched medium from modified Maxwell's equations with streched coordinates," *Microwave and Optical Technology Letters*, Vol. 7, No. 13, 599–604, 1994.

9. Kancleris, Ž., V. Tamošiūnas, and M. Tamošiūniene, "Computation of the averaged electric field in the semiconductor obstacle placed in the coaxial line," *Journal of Electromagnetic Waves and Applications*, Vol. 20, No. 4, 447–460, 2006.

10. Chen, Q. and V. Fusco, "Three dimensional cylindrical coordinate finite difference time domain analysis of curved slot line," *2nd Int. Conf. Computations in Electromag.*, 323–326, U.K., 1994.

11. Chen, Y., R. Mittra, and P. Harms, "Finite-difference time-domain algorithm for solving Maxwell's equation in rotationally symmetric geometries," *IEEE Trans. Microwave Theory Tech.*, Vol. 44, No. 6, 832–839, 1996.

12. Dib, N., T. Weller, M. Scardeletti, and M. Imparato, "Analysis of cylindrical transmission lines with the finite-difference time-domain method," *IEEE Trans. Microwave Theory Tech.*, Vol. 47, No. 4, 509–512, 1999.

13. Trakic, A., H. Wang, F. Liu, H. S. Lpez, and S. Crozier, "Analysis of transient eddy currents in MRI using a cylindrical FDTD method," *IEEE Trans. Appl. Supercond.*, Vol. 16, No. 9, 1924–1936, 2006.

14. Liu, F. and S. Crozier, "An FDTD model for calculation of gradient-induced eddy currents in MRI system," *IEEE Trans. Appl. Supercond.*, Vol. 14, No. 9, 1983–1989, 2004.

15. Kancleris, Ž., "Handling of singularity in finite-difference time-domain procedure for solving Maxwell's equations in cylindrical coordinate system," *IEEE Trans. on Antennas and Propagation*, Vol. 56, No. 2, 610–613, 2008.

16. Baskakov, S. I., "Basics of electrodynamics," *Sov. Radio*, Moscow, 1973 (in Russian).

17. Kancleris, Ž., G. Šlekas, V. Tamošiunas, R. Simniškis, P. Ragulis, and M. Tamošiūnienė, "Semiconductor plate interacting with TE$_{01}$ mode in circular waveguide," *Lithuanian J. Phys.*, Vol. 49, No. 1, 35–43, 2009.